Development 135, 1303-1313 (2008) doi:10.1242/dev.019075

PLK-1 asymmetry contributes to asynchronous cell division of *C. elegans* embryos

Yemima Budirahardja and Pierre Gönczy*

Acquisition of lineage-specific cell cycle duration is an important feature of metazoan development. In *Caenorhabditis elegans*, differences in cell cycle duration are already apparent in two-cell stage embryos, when the larger anterior blastomere AB divides before the smaller posterior blastomere P_1. This time difference is under the control of anterior-posterior (A-P) polarity cues set by the PAR proteins. The mechanisms by which these cues regulate the cell cycle machinery differentially in AB and P_1 are incompletely understood. Previous work established that retardation of P_1 cell division is due in part to preferential activation of an ATL-1/CHK-1 dependent checkpoint in P_1, but how the remaining time difference is controlled is not known. Here, we establish that differential timing relies also on a mechanism that promotes mitosis onset preferentially in AB. The polo-like kinase PLK-1, a positive regulator of mitotic entry, is distributed in an asymmetric manner in two-cell stage embryos, with more protein present in AB than in P_1. We find that PLK-1 asymmetry is regulated by A-P polarity cues through preferential protein retention in the embryo anterior. Importantly, mild inactivation of *plk-1* by RNAi delays entry into mitosis in P_1, but not in AB, in a manner that is independent of ATL-1/CHK-1. Together, our findings support a model in which differential timing of mitotic entry in *C. elegans* embryos relies on two complementary mechanisms: ATL-1/CHK-1-dependent preferential retardation in P_1 and PLK-1-dependent preferential promotion in AB, which together couple polarity cues and cell cycle progression during early development.

KEY WORDS: *C. elegans*, Embryo, Polo-like kinase, Asymmetry, Cell division timing

INTRODUCTION

Lineage specific cell cycle duration is crucial for metazoan development. For example, in *Drosophila* embryos, the expression pattern of the Cdc25 phosphatase *string* (*stg*) dictates the timing of the G2/M transition in different mitotic domains during the 14th cell cycle (Edgar and O'Farrell, 1990). *stg* mutant embryos arrest at the G2/M transition of cycle 14, whereas *stg* overexpression in interphase of cycle 14 leads to premature entry into mitosis and subsequent patterning defects (Edgar and O'Farrell, 1990). In *Xenopus*, both the Wee1 kinase and the Cdc25C phosphatase are essential for entry into mitosis and alterations in their levels result in morphogenesis defects (Murakami et al., 2004). Whereas these examples illustrate the importance of coupling cell division timing and embryonic development, in general the mechanisms underlying such coupling remain incompletely understood.

In *C. elegans*, a difference in cell cycle timing is apparent already in two-cell stage embryos, when the larger anterior blastomere AB divides ~2 minutes earlier than the smaller posterior blastomere P_1. As in early embryos of many species, the cell cycle is rapid and alternates between S and M phases in early embryos of *C. elegans*. Thus, the ~2 minutes time difference correspond to ~15% of the entire duration of the AB cell cycle. The asynchrony between AB and P_1 is entirely under the control of A-P polarity cues that are established by six PAR proteins and associated components, in concert with the actomyosin network (Aceto et al., 2006; Etemad-Moghadam et al., 1995; Guo and Kemphues, 1995; Guo and Kemphues, 1996; Levitan et al., 1994; Morton et al., 2002; Tabuse et al., 1998; Watts et al., 1996; Watts et al., 2000). When A-P polarity cues are defective, as for example in *par-2* or *par-3* mutant embryos, the first division is equal and the two resulting daughter cells enter mitosis in synchrony (Kemphues et al., 1988).

How A-P polarity cues control the asynchrony between AB and P_1 is only partially understood. An aspect of the answer lies in an ATL-1/CHK-1-dependent checkpoint that is activated preferentially in P_1, thus retarding entry into mitosis more in that blastomere and explaining ~40% of the time difference (Brauchle et al., 2003). Preferential checkpoint activation is largely abrogated in embryos that have normal A-P polarity, but which undergo an equal first cleavage following defective spindle positioning (Brauchle et al., 2003). These observations suggest that ATL-1/CHK-1 activation normally occurs preferentially in P_1 because this smaller blastomere inherits less of a rate-limiting component for DNA replication following unequal first cleavage (Brauchle et al., 2003). These findings indicate also that there must be an ATL-1/CHK-1 independent and size-independent mechanism that regulates the remaining ~60% time difference. Compatible with the existence of a size-independent mechanism, microsurgery experiments established that AB enters mitosis earlier even if it becomes smaller than P_1 because of the removal of cytoplasmic material (Schierenberg and Wood, 1985).

One attractive candidate for regulating the remaining time difference is the polo-like kinase PLK-1. First, Polo-like kinases 1 (Plk1) promote mitotic entry in several species (Abrieu et al., 1998; Lane and Nigg, 1996; Lenart et al., 2007; Sumara et al., 2004). Plk-1 is thought to act at this cell cycle transition by phosphorylating the Myt1 kinase and the Cdc25 phosphatase. As a result, Myt1 is inactivated and Cdc25 is activated, which together promotes activation of Cdk1 and entry into mitosis (Inoue and Sagata, 2005; Kumagai and Dunphy, 1996; Qian et al., 2001; Roshak et al., 2000). In *C. elegans*, PLK-1 is also essential for M phase entry. Oocytes in *plk-1(RNAi)* animals fail to undergo nuclear envelope breakdown (NEDB) and do not complete the meiotic divisions (Chase et al., 2000). As anticipated, this phenotype is identical to that observed after RNAi-mediated inactivation of NCC-1, the Cdk1 homolog

Swiss Institute for Experimental Cancer Research (ISREC), School of Life Sciences, Swiss Federal Institute of Technology (EPFL), Lausanne, Switzerland.

*Author for correspondence (e-mail: pierre.gonczy@epfl.ch)

Accepted 31 January 2008

acting during the meiotic and the mitotic divisions in early *C. elegans* development (Boxem et al., 1999). A second reason for considering PLK-1 as an attractive candidate for regulating the remaining time difference between AB and P_1 is that examination of published data reporting the distribution of PLK-1 using N-terminal peptide antibodies (Chase et al., 2000) indicates that PLK-1 is more abundant in AB than in P_1. Therefore, we set out to investigate whether PLK-1 plays a role in regulating the asynchrony between AB and P_1 by promoting entry into mitosis preferentially in AB.

MATERIALS AND METHODS

Nematode strains and RNA-mediated inactivation

Transgenic worms expressing GFP-PAR-2 (Cuenca et al., 2003), GFP-PLK-1 (Leidel and Gönczy, 2003) or GFP-HIS-11 (Histone 2B) (Praitis et al., 2001) were grown at 24°C. Mutants of genotypes *par-3*(*it71*) *unc-32(e189)/qC1* (Kemphues et al., 1988), *par-1*(*it51*) *rol-4(sc8)/DnT1* (Guo and Kemphues, 1995) and *pie-1*(*zu154*) *unc-25(e156)/qC1* (Tenenhaus et al., 1998) were grown at 20°C, whereas temperature-sensitive *par-4*(*it57*ts) mutants (Morton et al., 1992) were grown at 15°C and shifted to 25°C for 24 hours before analysis.

The *atl-1*(*tm853*) deletion allele was obtained from the National Bioresource Project, Japan. We balanced the mutation using nT1[GFP-MYO-2 *unc-56*] and genotyped the animals by PCR using *atl-1* specific primers. *atl-1*(*tm853*) is probably a null allele because it harbors a 720 bp deletion that creates a frameshift and results in a premature stop codon (Garcia-Muse and Boulton, 2005). We found that homozyous mutant *atl-1*(*tm853*) animals are fertile, but give rise only to dead embryos, as reported previously (Garcia-Muse and Boulton, 2005).

RNAi-mediated inactivation using bacterial feeding strain of *plk-1* (covering nucleotides 890 to 1887 of the *plk-1* cDNA) were performed as follows: for examining the specificity of PLK-1 C-terminal antibodies (Fig. 1B,G), L4 larvae were selected and feeding performed for 15 hours at 20°C; for partial depletion to measure PLK-1 ratio in AB versus P_1 (Fig. 2E,F), young adult worms were selected and feeding performed for 8 hours at 20°C; for mild inactivation whereby entry into mitosis is delayed only in P_1 (Fig. 6B, Fig. 7G; see Fig. S1B,D in the supplementary material), young adult worms were selected and feeding performed for 6 hours at 20°C. Other RNAi-mediated inactivation experiments were performed by selecting L4 larvae and feeding them as follows: *par-5*(*RNAi*), *par-2*(*RNAi*) and *zen-4*(*RNAi*), 24 hours at 20°C; *div-1*(*RNAi*) (Brauchle et al., 2003), 26 hours at 20°C; *tba-2*(*RNAi*) (Sonneville and Gönczy, 2004) and *nmy-2*(*RNAi*) (Guo and Kemphues, 1995), 24 hours at 24°C; and *goa-1*/*gpa-16*(*RNAi*) (Colombo et al., 2003), 48 hours at 20°C. Bacterial RNAi feeding strains for *par-2* and *zen-4* were from the Ahringer collection (Kamath et al., 2003) and that for *par-5* from the Vidal collection (Rual et al., 2004).

PLK-1 C-terminal antibodies

The last 159 bp of the *plk-1*-coding region were cloned into pGEX-6P-2 (Amersham Biosciences). The resulting fusion protein was expressed, column-purified using Glutathione Sepharose 4 Fast Flow resin (Amersham Biosciences), eluted with 20 mM reduced glutathione pH 7.5, dialyzed and injected into a rabbit (Eurogentec). For affinity purification, the same fragment was cloned into pMAL-p2E (NEB). The resulting fusion protein was expressed, column-purified using amylose resin (NEB), eluted with 20 mM maltose, dialyzed and coupled to affigel resin (BioRad). The serum was purified on this column, eluted with 0.2 M glycine pH 2.2 in 0.5 M NaCl, dialyzed against PBS containing 8.7% glycerol and stored at –20°C in 50% glycerol. The final concentration of PLK-1 antibodies is 1 μg/μl.

SDS-PAGE and western blot analyses were carried out according to standard procedures. Rabbit anti-PLK-1 C terminal and mouse anti-α tubulin antibodies were used at 1/1000 and the HRP-conjugated goat anti-rabbit and anti-mouse secondary antibodies (Promega) at 1/5000; the signal was revealed with standard chemiluminesence (Roche).

Indirect immunofluorescence

Fixation and indirect immunofluorescence were performed essentially as described (Gönczy et al., 1999). The following primary mouse antibodies were used: α-tubulin (DM1A, Sigma; 1/200) and GFP (MAB3580, Chemicon; 1/200, to detect GFP-PAR-2). The following primary rabbit antibodies were used: PLK-1 C-terminal fusion protein (1/500; this study), GFP (a gift from Viesturs Simanis; 1/300, to detect GFP-PLK-1), NCC-1 (a gift from Andy Golden; 1/1000) and phospho-specific tyrosine 15 (pT15) antibody to detect NCC-1 phosphorylation (Calbiochem, 1/100). Secondary antibodies were goat anti-mouse coupled to Alexa 488 (1/500) and goat anti-rabbit coupled to Alexa 568 (1/1000) (Molecular Probes). Slides were counterstained with ~1 μg/ml Hoechst 33258 (Sigma) to reveal DNA. Images were taken on a LSM510 Zeiss confocal microscope. For quantification of the ratio of PLK-1 in AB versus P_1, images were taken in the linear intensity range with a 63× lens on a Zeiss Axioplan 2 microscope equipped with a 12-bit Diagnostic Instrument Spot RT cooled CCD camera and analyzed using MetaMorph software. For pT15 staining, 20 confocal sections encompassing the AB and P_1 nuclei were taken every 0.45 μm with a 63× objective and the maximum intensity projection was constructed using ImageJ.

FRAP experiments and image analysis

FRAP was performed on an LSM510 Meta Zeiss confocal microscope, acquiring one image every 10 seconds at each time point using a 63× lens, with zoom 2, average 2 and unidirectional scanning of 512×512 pixels at 9% laser power, resulting in acquisition times of ~800 mseconds. For photobleaching, the whole anterior or posterior half of a metaphase one-cell stage GFP-PLK-1 embryo was bleached with 30 iterations at 100% laser power. The data were analyzed using ImageJ by measuring the average intensity of the anterior or posterior cytoplasmic area, excluding centrosomes and kinetochores, whose frequent movements could generate measurement errors. The intensity in the embryo anterior in the five images before photobleaching was averaged and assigned a value of 1, whereas the intensity in the bleached area just after photobleaching was assigned a value of 0.

Time-lapse microscopy

Embryos were analyzed by time-lapse DIC microscopy at ~23°C as described (Gönczy et al., 1999). The timing of cytokinesis in P_0 (measured at the time of cleavage furrow initiation) as well as that of NEBD in AB and P_1 (measured at the time of nuclear membrane disappearance) were determined. The time separating cytokinesis in P_0 from NEBD in either AB or P_1 corresponds to interphase.

Embryos expressing GFP-Histone 2B were imaged using dual time-lapse fluorescent and DIC microscopy as described (Brauchle et al., 2003), and the timing of the metaphase to anaphase transition determined in P_0, AB and P_1.

Quantification of PLK-1 levels

PLK-1 levels were quantified in fixed wild-type, *par-2*(*RNAi*) and *par-3*(*it71*) embryos. To obtain reliable values, we normalized cytoplasmic PLK-1 levels with respect to centrosomal PLK-1 levels in the same embryo. Moreover, the analysis was conducted in metaphase and early anaphase one-cell stage embryos because the centrosomal signal is strong and reproducible at these stages, and because anterior and posterior levels can be quantified simultaneously in the same cell. As PLK-1 is distributed symmetrically in *par-2*(*RNAi*) and *par-3*(*it71*) embryos, PLK-1 levels in the anterior and the posterior were averaged in these cases. Embryos which were partially stained or subjected to incomplete RNAi-mediated inactivation of *par-2* were not considered.

RESULTS

PLK-1 is distributed asymmetrically in early *C. elegans* embryos

To investigate whether the asymmetry in PLK-1 distribution that is apparent in a published report (Chase et al., 2000) reflects bona fide PLK-1 distribution, and not merely that of a particular epitope, we raised and affinity-purified polyclonal antibodies against a C-terminal fragment of the protein (Fig. 1A). These antibodies recognize a single band at the expected size of ~70 kDa in wild-type embryonic extracts by western blot analysis (Fig. 1B, lane 1). This

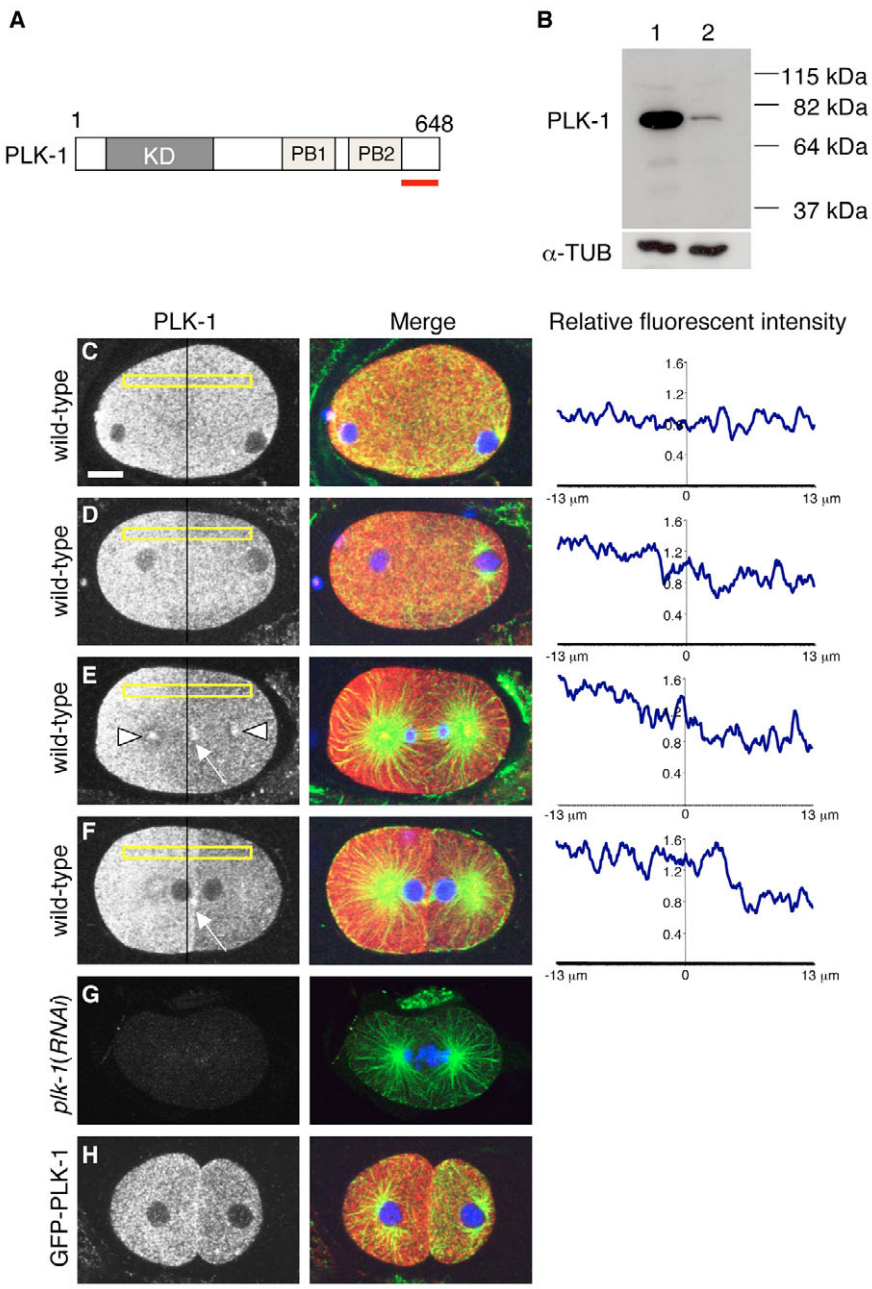

Fig. 1. PLK-1 is distributed asymmetrically in early *C. elegans* embryos. (**A**) Schematic representation of *C. elegans* PLK-1. The kinase (KD) and polo boxes (PB1 and PB2) are indicated, as is the region against which the C-terminal antibodies were raised (amino acids 589-648; underlined in red). (**B**) Western blot of wild-type (lane 1) and strong *plk-1*(*RNAi*) (lane 2) embryonic extracts probed with PLK-1 antibodies, which recognize a specific band at the expected size of ~70 kDa. The blot was reprobed with α-tubulin antibodies as a loading control. (**C-H**) Wild-type (C-F), strong *plk-1*(*RNAi*) (G) or GFP-PLK-1 (H) embryos stained for PLK-1 (C-G) or GFP (H) (shown alone in the left panels and in red in the merged panels), α-tubulin (green) and DNA (blue). In all figures, anterior is towards the left and scale bars correspond to 10 μm. Line scans of PLK-1 intensity of C-F (yellow rectangles) are shown on the right, with 1.0 corresponding to the average pixel intensity within the rectangle. (C) Shortly after the completion of meiosis, PLK-1 distribution in the cytoplasm is uniform. (D) In early prophase, cytoplasmic PLK-1 becomes asymmetric, with more protein present in the anterior. (E,F) PLK-1 asymmetry is maintained in anaphase (E) and in the early two-cell stage (F). PLK-1 is enriched at centrosomes (E, arrowheads) and the midbody (E,F, arrows). The signal detected by PLK-1 antibodies is specific, as it is essentially absent in strong *plk-1*(*RNAi*) embryos (G), which nevertheless allowed passage through the meiotic divisions in this particular embryo. Finally, asymmetric distribution in two-cell stage embryos is also apparent with GFP-PLK-1 (H). The fact that asymmetry with this particular transgenic line is less pronounced than that of endogenous PLK-1 may reflect the fact that excess GFP-PLK-1 cannot be efficiently retained at the anterior in the presence of endogenous PLK-1. Compatible with this view, anterior enrichment of GFP-PLK-1 to an extent comparable to that of endogenous PLK-1 was observed with a distinct transgenic line (a gift from Asako Sugimoto) that expresses lower protein levels (data not shown).

band is significantly reduced in *plk-1*(*RNAi*) embryonic extracts, demonstrating specificity (Fig. 1B, lane 2). We used these antibodies to examine PLK-1 distribution in early *C. elegans* embryos. As shown in Fig. 1C, we found that PLK-1 is distributed in a uniform manner in the cytoplasm just after meiotic exit. PLK-1 distribution becomes asymmetric shortly thereafter, with more protein present on the anterior side of the embryo (Fig. 1D). This asymmetry persists throughout the one-cell stage and until the end of the two-cell stage (Fig. 1E,F; data not shown). Line scans quantifying pixel intensities confirm these observations (Fig. 1C-F). These antibodies also label centrosomes (Fig. 1E, arrowheads), the midbody (Fig. 1E,F, arrows) and kinetochores (data not shown), as reported previously (Chase et al., 2000). The signals detected by these antibodies in wild-type embryos are absent from embryos depleted of PLK-1 by RNAi (Fig. 1G), demonstrating specificity. We found an analogous distribution using antibodies directed against GFP in transgenic animals expressing GFP-PLK-1, although the asymmetry is somewhat less pronounced in this case (Fig. 1H).

Overall, these observations lead us to conclude that PLK-1 distribution is asymmetric in one- and two-cell stage *C. elegans* embryos, with more protein being present on the anterior side.

Achieving PLK-1 asymmetry

We next set out to investigate how PLK-1 asymmetry is achieved. We first addressed whether the underlying mechanism is active solely in the one-cell stage and results in asymmetry at the two-cell stage merely because the first cleavage separates the anterior and posterior pools of PLK-1. Alternatively, the mechanism at the root of PLK-1 asymmetry could be active also during the second cell cycle. To distinguish between these possibilities, we examined PLK-1 asymmetry at the second cell cycle in *zen-4*(*RNAi*) embryos, which

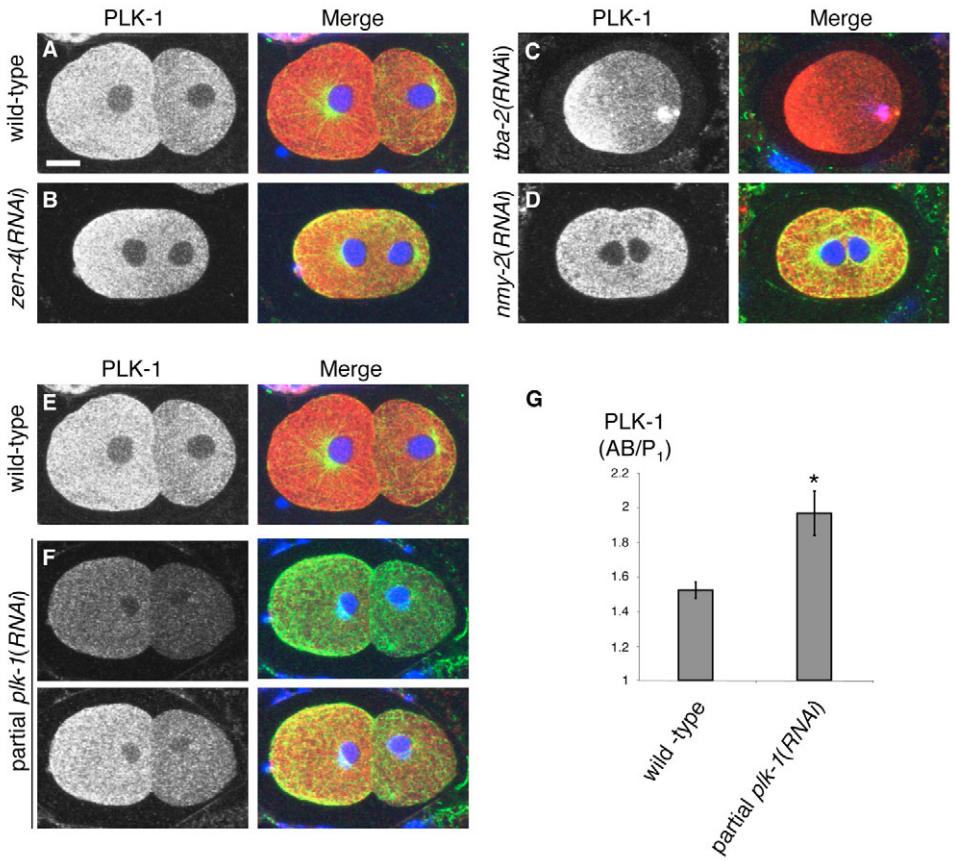

Fig. 2. Achieving PLK-1 asymmetry. (**A-D**) Wild-type (A), *zen-4*(*RNAi*) (B), *tba-2*(*RNAi*) (C) or *nmy-2*(*RNAi*) (D) embryos stained for PLK-1 (shown alone in the left panels and in red in the merged panels), α-tubulin (green) and DNA (blue). PLK-1 asymmetry is maintained despite cytokinesis failure (B). Whereas microtubules are not essential for PLK-1 asymmetry as the asymmetry is maintained and even slightly increased upon α-tubulin depletion (C), the actomyosin network is needed (D). (**E**,**F**) Wild-type (E) and partial *plk-1*(*RNAi*) (F) embryos stained for PLK-1 (shown alone in the left panels and in red in the merged panels), α-tubulin (green) and DNA (blue). Overall PLK-1 levels are diminished in partial *plk-1*(*RNAi*) embryos (F, top panel). To better illustrate the alteration in ratio between AB and P_1, a second image of the same partial *plk-1*(*RNAi*) embryo is shown (F, bottom panel), in which intensities were increased so as to match those in AB in the wild-type embryo. (**G**) Average ratios, along with s.e.m., of PLK-1 in AB versus P_1 in wild-type and partial *plk-1*(*RNAi*) embryos stained as in E and F. Wild type, 1.52±0.05, n=64; partial *plk-1*(*RNAi*), 1.97±0.13, n=16. Student's t-test, $P=2.6\times10^{-11}$. The star indicates that the difference with wild type is statistically significant.

are defective in cytokinesis (Raich et al., 1998). As shown in Fig. 2B, PLK-1 asymmetry is still apparent in such embryos, demonstrating that PLK-1 asymmetry is maintained during the second cell cycle.

We then tested whether the microtubule cytoskeleton or the actomyosin network is required for PLK-1 asymmetry. To test the role of microtubules, we depleted α-tubulin using *tba-2*(*RNAi*) (Sonneville and Gönczy, 2004). We found that PLK-1 asymmetry is still apparent and even slightly accentuated in *tba-2*(*RNAi*) embryos (Fig. 2C), indicating that microtubules are dispensable for PLK-1 asymmetry. To examine the role of the actomyosin network, we depleted the non-muscle myosin II NMY-2 (Guo and Kemphues, 1995). As shown in Fig. 2D, PLK-1 asymmetry is abolished in *nmy-2*(*RNAi*) embryos, indicating that the actomyosin network is required, directly or indirectly, for PLK-1 asymmetry.

A fraction of PLK-1 is retained at the embryo anterior

Next, we considered whether PLK-1 distribution is asymmetric because a fraction of the protein is retained in the embryo anterior. To test this possibility, we designed a Fluorescence Recovery After Photobleaching (FRAP) experiment to probe the mobility of the posterior and anterior pools of PLK-1. To probe the mobility of GFP-PLK-1 located in the embryo posterior, we photobleached the anterior half of the embryo and assayed fluorescence intensity over time in both posterior and anterior halves (Fig. 3A,B). We found that the posterior pool of GFP-PLK-1 moves readily into the anterior half, such that fluorescence intensity in the two halves equilibrates ~90 seconds after photobleaching (Fig. 3B). Conversely, to probe the mobility of GFP-PLK-1 located into the anterior, we photobleached the posterior half of the embryo and similarly assayed fluorescence intensity (Fig. 3C,D). Importantly, we found in this case that even though the bulk of the anterior pool of GFP-PLK-1 moves readily into the posterior half, a fraction of GFP-PLK-1 is retained in the embryo anterior, such that fluorescence intensity in the two halves remains different at 90 seconds after photobleaching and thereafter (Fig. 3D).

As PLK-1 can be retained in the embryo anterior, we reasoned that the extent of asymmetry may increase when overall PLK-1 levels are diminished, because the remaining protein would be preferentially retained in the anterior, leaving less protein left for the posterior. To test this possibility, we compared the ratio of PLK-1 in AB versus P_1 in the wild type with that observed after partial RNAi-

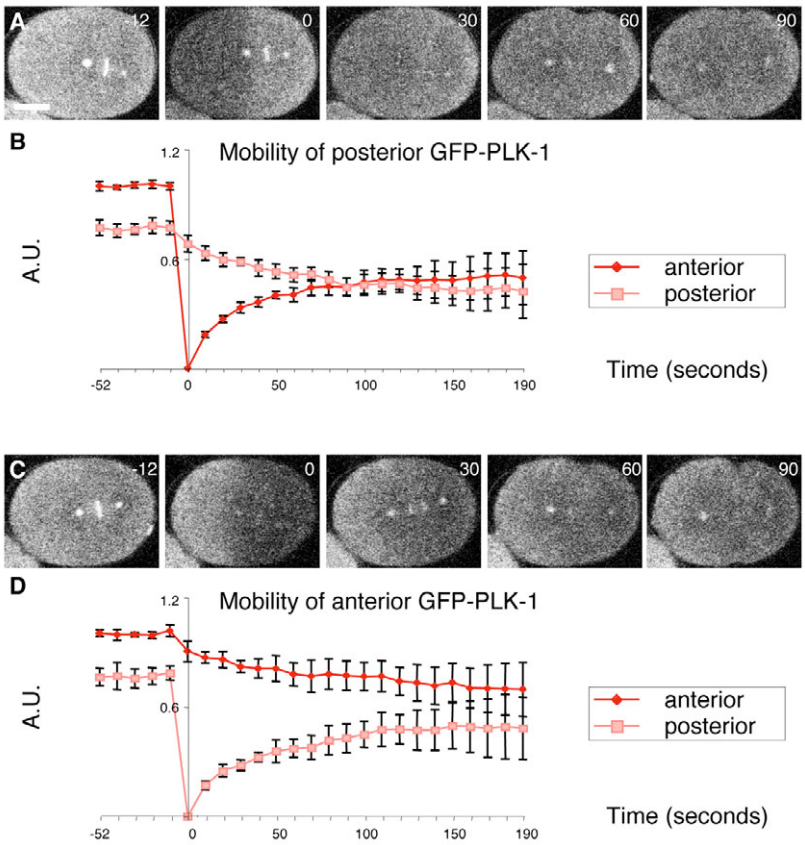

Fig. 3. Anterior retention of PLK-1. (**A**,**C**) Confocal images of GFP-PLK-1 embryos before photobleaching (first panels), immediately after photobleaching the anterior half (A, second panel) or the posterior half (C, second panel) and three time intervals afterwards (third to fifth panels). Time elapsed is indicated in seconds with 0 corresponding to the end of photobleaching. (**B**,**D**) GFP-PLK-1 relative intensity ±s.e.m. plotted as a function of time, both for anterior (B, *n*=5) and posterior (D, *n*=7) photobleaching. Five images before photobleaching and 20 images afterwards were captured every 10 seconds, except for the images captured immediately after photobleaching, which were captured 12 seconds after the previous one. GFP-PLK-1 movement from the posterior to the anterior rapidly results in uniform GFP-PLK-1 distribution (B), whereas movement from the anterior to the posterior does not, leaving GFP-PLK-1 distribution asymmetric (D).

mediated inactivation of PLK-1. We found this ratio to be 1.52±0.05 in the wild-type (Fig. 2E,G) and 1.97±0.13 in embryos partially depleted of PLK-1 (Fig. 2F,G). Although more complex mechanisms can be envisaged, this increase in ratio, together with the outcome of the FRAP experiment, is compatible with a model in which PLK-1 asymmetry is achieved through protein retention in the embryo anterior.

PLK-1 asymmetry is controlled by A-P polarity cues

As the time difference between AB and P_1 is entirely under the control of A-P polarity cues (Kemphues et al., 1988), if PLK-1 were to play a role in controlling this time difference, then PLK-1 asymmetry should be regulated by polarity cues. To address this possibility, we first examined when PLK-1 becomes asymmetric with respect to establishment of A-P polarity. Using GFP-PAR-2 as a polarity marker, we found that PLK-1 distribution becomes asymmetric shortly after polarity establishment (Fig. 4A,B), compatible with PLK-1 asymmetry being regulated by A-P polarity cues. To test whether this is the case, we examined PLK-1 distribution in embryos with impaired PAR-1, PAR-2, PAR-3, PAR-4 or PAR-5 function. Importantly, we found that PLK-1 distribution is symmetric in such embryos (Fig. 4D-H). Similarly, PLK-1 distribution is symmetric in *pkc-3*(*RNAi*) and *mex-5/6*(*RNAi*) embryos, which also have defective A-P polarity (Cuenca et al., 2003; Tabuse et al., 1998) (data not shown). Therefore, we conclude that PLK-1 asymmetry is regulated by A-P polarity cues.

We then investigated whether polarity cues regulate PLK-1 asymmetry separately from asymmetric spindle positioning and cell fate determination, both of which are also controlled by A-P polarity (reviewed by Gönczy and Rose, 2005). To this end, we examined *goa-1*/*gpa-16*(*RNAi*) embryos, in which the first division is equal as a result of symmetric spindle positioning (Colombo et al., 2003; Gotta and Ahringer, 2001), as well as *pie-1*(*zu154*) mutant embryos, in which the fate of the P_1 blastomere is altered (Tenenhaus et al., 1998; Tenenhaus et al., 2001). We found that PLK-1 distribution is asymmetric in such embryos (Fig. 4I,J), indicating that A-P polarity cues regulate PLK-1 asymmetry separately from spindle positioning and cell fate determination.

PLK-1 levels correlate with the timing of mitotic entry upon PAR-2 and PAR-3 inactivation

We set out to test whether PLK-1 levels are important for dictating the timing of mitosis onset. We reasoned that an analysis of PLK-1 levels and mitotic timing in embryos depleted of PAR-2 and PAR-3 may shed light on this issue. In the absence of PAR-2, both blastomeres at the two-cell stage resemble AB in terms of spindle orientiation and cortical marker distribution (Boyd et al., 1996; Kemphues et al., 1988). Conversely, in the absence of PAR-3, both blastomeres resemble P_1 in these respects (Etemad-Moghadam et al., 1995; Kemphues et al., 1988). Accordingly, we found that the timing of mitotic entry of both blastomeres in *par-2*(*RNAi*) embryos resembles most that of AB in the wild type, whereas the timing of both blastomeres in *par-3*(*it71*) mutant embryos is similar to that of P_1 in the wild-type (Fig. 5A-F; see Table S1 and Movies 1-4 in the supplementary material). Quantification of fixed specimens established that PLK-1 levels in *par-2*(*RNAi*) embryos are similar to those in the anterior of wild-type embryos, whereas those in *par-3*(*it71*) embryos are similar to those in the posterior of wild-type embryos (Fig. 5G). We conclude that levels of PLK-1 correlate with the timing of mitotic entry upon depletion of PAR-2 and PAR-3.

PLK-1 asymmetry contributes to asynchronous entry into mitosis in AB and P_1

We next set out to address whether the asymmetric distribution of PLK-1 is important for asynchronous division of AB and P_1. Strong RNAi-mediated inactivation of *plk-1* prevents completion of the meiotic divisions (Chase et al., 2000) and conditional mutant alleles are not available, precluding an analysis in two-cell stage embryos using strong reduction of function conditions. Thus, we performed partial *plk-1*(*RNAi*) and analyzed cell cycle progression using time-lapse DIC microscopy. We found that mitotic entry in partial *plk-1*(*RNAi*) embryos is delayed somewhat in AB, but more extensively in P_1, resulting in a significant increase in the ratio of the duration of interphase in P_1 over the duration of interphase in AB (RI) (see Tables S1 and S2 in the supplementary material). Although this observation indicates that PLK-1 levels are crucial for timely entry into mitosis, chromosomes are often mis-segregated in these partial *plk-1*(*RNAi*) embryos, which in theory could contribute to altering cell cycle progression. Therefore, we conducted yet milder RNAi-mediated inactivation of *plk-1*, such that chromosome segregation defects are not observed. Importantly, we found that whereas the timing of cell cycle progression in AB is not affected in these mild *plk-1*(*RNAi*) embryos, entry into mitosis is delayed in P_1 (Fig. 6A-B; see Table S1, Movies 5 and 6 in the supplementary material). As a result, RI is increased compared with the wild type (Fig. 6E; see Table S2 in the supplementary material). To corroborate these observations, we analyzed the timing of events in embryos expressing GFP-Histone 2B to monitor precisely the metaphase to anaphase transition. We found again that whereas cell cycle duration is not perturbed in AB in mild *plk-1*(*RNAi*) embryos, a delay is observed in P_1 (see Fig. S1A,B, and Movies 11 and 12 in the supplementary material), resulting in an increased ratio of cell cycle duration in P_1 over that in AB (see Fig. S1E and Table S3 in the supplementary material). As P_1 has lower levels of PLK-1 than AB in the wild type, it is presumably more sensitive to PLK-1 diminution, accounting for the observed increased asynchrony upon mild RNAi-mediated depletion. Taken together, these results suggest that PLK-1 levels are important for timing mitotic entry and that PLK-1 asymmetry contributes to the asynchronous division of AB and P_1.

As PLK-1 promotes mitotic entry by ultimately activating the Cdk1 NCC-1, we anticipated that interfering with NCC-1 function may have consequences on differential cell cycle duration resembling those observed in mild *plk-1*(*RNAi*) embryos. NCC-1 is distributed symmetrically in AB and P_1 (see Fig. S2A-C in the supplementary material) (Boxem et al., 1999), but is activated first in AB, as evidenced by the fact that phospho-specific antibodies that recognize the inactive form of NCC-1 disappear first from AB (see Fig. S2D-F in the supplementary material) (Hachet et al., 2007). As anticipated, we found that entry into mitosis in mild *ncc-1*(*RNAi*) embryos is delayed to a larger extent in P_1 than in AB (Fig. 6C; see Table S1 and Movie 7 in the supplementary material), resulting in an increased RI compared with the wild type (Fig. 6E; see Table S2

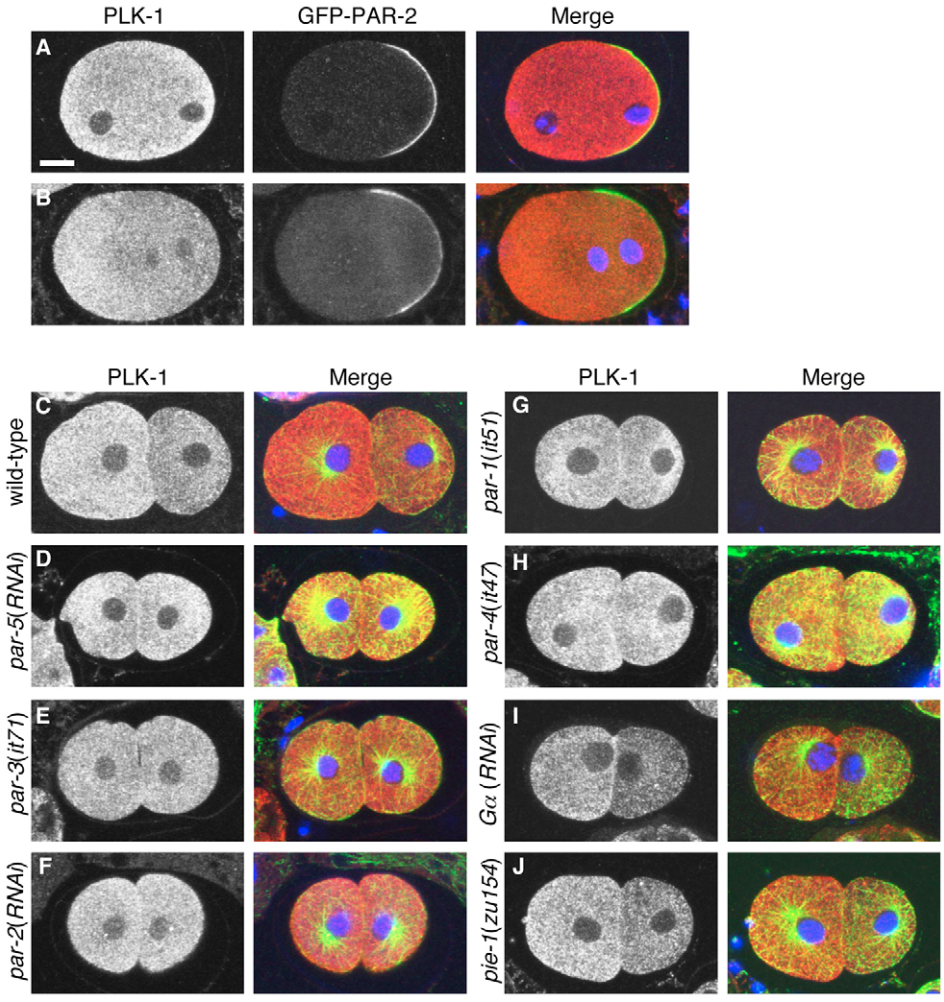

Fig. 4. PLK-1 asymmetry is controlled by A-P polarity cues. (**A**,**B**) GFP-PAR-2 embryos stained for PLK-1 (shown alone in the left panels and in red in the merged panels), GFP (shown alone in the middle panels and in green in the merged panels) and DNA (blue). The posterior domain of GFP-PAR-2 is established before PLK-1 distribution becomes asymmetric. (**C-J**) Embryos of the indicated genotypes stained for PLK-1 (shown alone in the left panels and in red in the merged panels), α-tubulin (green) and DNA (blue). PLK-1 asymmetry is dependent on the PAR proteins (D-H), but not on GOA-1/GPA-16 (collectively referred to as Gα) or PIE-1 (I,J).

in the supplementary material), reminiscent of the increase observed in mild *plk-1*(*RNAi*) embryos. Even though in principle factors other than PLK-1 could be responsible for differential activation of NCC-1, this phenotypic similarity is compatible with the notion that PLK-1 asymmetry results in differential NCC-1 activation.

To address whether such a differential impact on mitotic entry in AB and P_1 is a general feature of slowing cell cycle progression, we analyzed embryos depleted of ATP-2, a β subunit of the catalytic moiety of ATP synthase (Tsang et al., 2001). Although cell cycle progression is considerably slower overall than in the wild-type, we found that mitotic entry is delayed to the same extent in AB and P_1 in *atp-2*(*RNAi*) embryos (Fig. 6D; see Table S1 and Movie 8 in the supplementary material), such that RI is indistinguishable from the wild type (Fig. 6E; see Table S2 in the supplementary material). Taken together, these results indicate that mild depletion of PLK-1 or of the downstream Cdk1 kinase NCC-1, but not any delay in cell cycle progression, retards entry into mitosis preferentially in P_1.

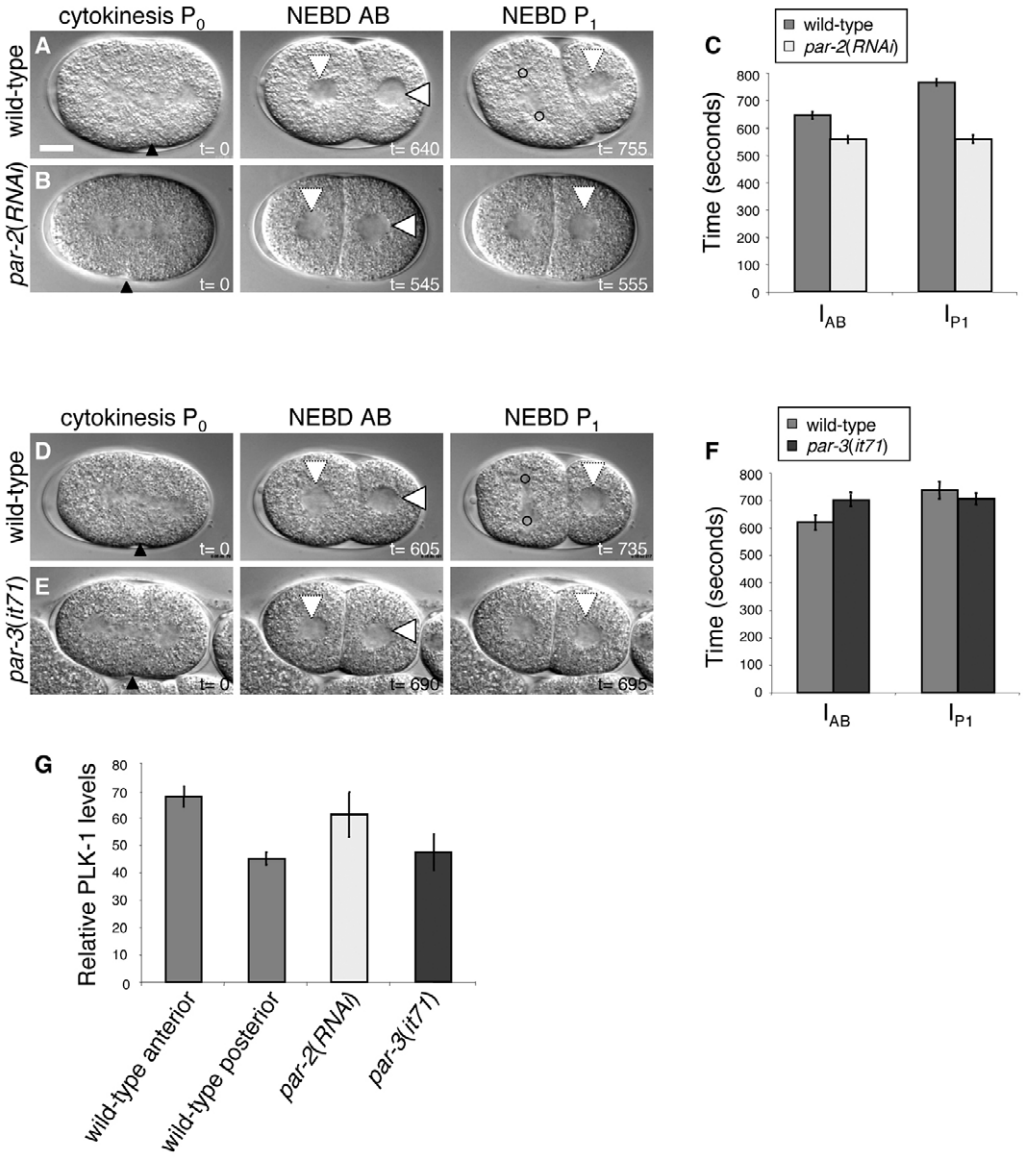

Fig. 5. PLK-1 levels correlate with the timing of mitotic entry after *par-2* or *par-3* inactivation. (**A**,**B**,**D**,**E**) Images from DIC time-lapse microscopy of wild-type (A,D), *par-2*(*RNAi*) (B) or *par-3*(*it71*) embryos (E) (see corresponding Movies 1-4). Black arrowheads indicate cleavage furrow ingression; white arrowheads with intact outline indicate intact nuclei; white arrowheads with broken outline indicate nuclei undergoing NEBD, which is apparent by loss of the smooth line corresponding to the nuclear envelope; circles indicate centrosomes in AB, the separation of which gives an indication of the advancement of mitosis. Cleavage furrow ingression at the onset of cytokinesis in P_0 is defined as t=0, and the time after that is indicated in seconds. (**C**,**F**) Average duration of interphase ±s.e.m. in AB and P_1 in wild-type and *par-2*(*RNAi*) (C) or wild-type and *par-3*(*it71*) (F) embryos. See Table S1 in the supplementary material for numerical values and statistical analysis. (**G**) Relative PLK-1 levels ±s.e.m. in anterior and posterior of one-cell stage wild-type, *par-2*(*RNAi*) and *par-3*(*it71*) embryos. Wild-type anterior, 0.68±0.04, n=12; wild-type posterior, 0.45±0.03, n=12; *par-2*(*RNAi*), 0.61±0.08, n=9; *par-3*(*it71*), 0.47±0.06, n=7. Student's t-test for wild-type anterior and *par-2*(*RNAi*), P=0.1; for wild-type posterior and *par-2*(*RNAi*), $P=1.7\times10^{-4}$; for wild-type anterior and *par-3*(*it71*), $P=7.36\times10^{-7}$; for wild-type posterior and *par-3*(*it71*), P=0.42. PLK-1 levels in *par-2*(*RNAi*) embryos are similar to those of the wild-type anterior, whereas PLK-1 levels in *par-3*(*it71*) are similar to those of the wild-type posterior.

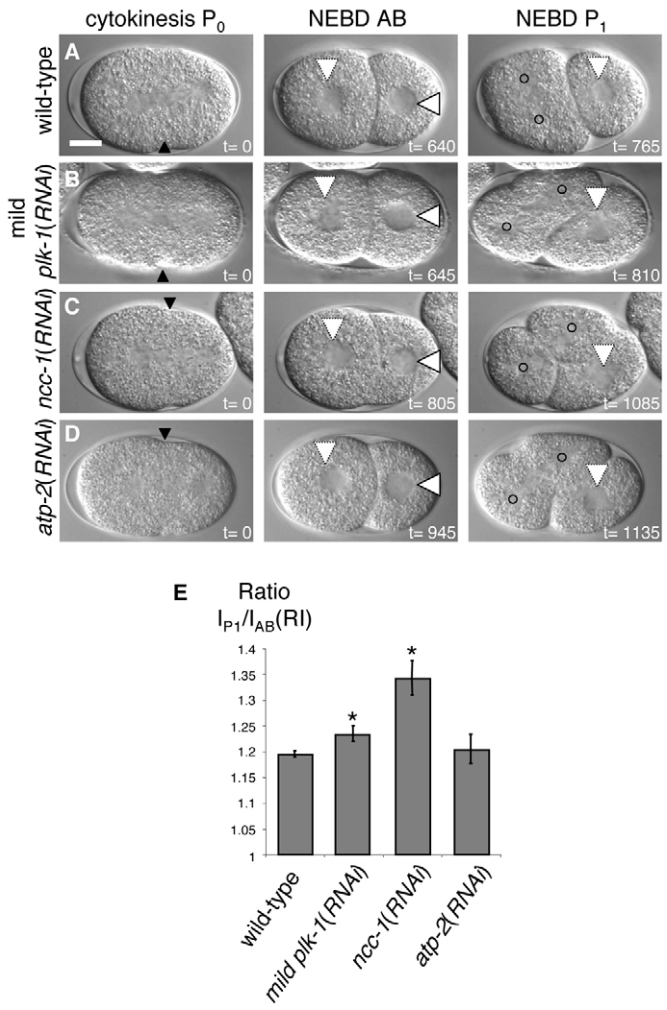

Fig. 6. PLK-1 contributes to differential timing of mitotic entry in AB and P_1. (**A-D**) Images from DIC time-lapse microscopy of wild-type (A), mild *plk-1*(*RNAi*) (B), *ncc-1*(*RNAi*) (C) and *atp-2*(*RNAi*) (D) (see corresponding Movies 5-8 in the supplementary material). See Fig. 5 legend for explanation of symbols and timing. (**E**) Average ratios ±s.e.m. of the duration of interphase in P_1 over the duration of interphase in AB [$(l_{P1})/(l_{AB})$] (RI) in embryos of the indicated genotypes. The star indicates that the difference with wild type is statistically significant. See Tables S1, S2 in the supplementary material for numerical values and statistical analysis.

PLK-1-mediated differential timing is independent of ATL-1

As differential timing in AB and P_1 is known to rely in part on preferential retardation of mitotic entry in P_1 through activation of an ATL-1/CHK-1 dependent checkpoint (Brauchle et al., 2003), we investigated whether the impact of PLK-1 depends on this checkpoint.

First, we addressed whether ATL-1/CHK-1 regulates PLK-1 asymmetric distribution. We examined the ratio of PLK-1 in AB versus P_1 in *atl-1*(*tm853*) embryos, which are checkpoint defective and thus have decreased RI (Fig. 7F,H; see Table S2 and Movie 9 in the supplementary material) (Brauchle et al., 2003), as well as in *div-1*(*RNAi*) embryos, which engage this checkpoint more than in the wild type owing to defective DNA replication and thus exhibit increased RI (Brauchle et al., 2003; Encalada et al., 2000). If ATL-1/CHK-1 regulates PLK-1 asymmetry, then the ratio of PLK-1 in AB versus P_1 should decrease in *atl-1*(*tm853*) embryos and increase in *div-1*(*RNAi*) embryos. We found instead that PLK-1 asymmetry is indistinguishable from the wild type in both cases (Fig. 7A-D), demonstrating that alterations in checkpoint signaling do not affect PLK-1 asymmetry.

To address unambiguously whether PLK-1 functions independently of ATL-1/CHK-1, we compared *atl-1*(*tm853*) embryos with *atl-1*(*tm853*) embryos treated with mild *plk-1*(*RNAi*). If the impact of PLK-1 on cell cycle progression requires ATL-1/CHK-1 function, then mild *plk-1*(*RNAi*) should not alter the timing of events observed in *atl-1*(*tm853*) embryos. In contrast to this prediction, however, we found that mild *plk-1*(*RNAi*) treatment of *atl-1*(*tm853*) embryos retards entry into mitosis in P_1 and thus increases RI compared with *atl-1*(*tm853*) mutant embryos (Fig. 7G,H; see Table S2 and Movie 10 in the supplementary material), as expected if the impact of PLK-1 is independent of ATL-1/CHK-1. To corroborate these observations, we conducted analogous experiments in embryos expressing GFP-Histone 2B. As reported in Fig. S1C-E in the supplementary material, these experiments similarly established that mild *plk-1*(*RNAi*) in *atl-1*(*tm853*) mutant embryos retards entry into mitosis in P_1 and thus increases RI compared with *atl-1*(*tm853*) mutant embryos (see Table S3, and Movies 13 and 14 in the supplementary material).

Taken together, these results establish that the impact of PLK-1 asymmetry on differential timing of mitotic entry in AB and in P_1 does not invoke ATL-1/CHK-1.

DISCUSSION

How cell cycle progression is modulated during development remains incompletely understood. Here, we demonstrate that asymmetric distribution of the cell cycle regulator PLK-1 couples A-P polarity cues to the timing of mitosis in two-cell stage *C. elegans* embryos.

Mechanisms underlying PLK-1 asymmetry

How is PLK-1 asymmetry established? In principle, asymmetry could result from *plk-1* mRNA being enriched at the embryo anterior. This does not appear to be the case, however, because mRNA localization is typically mediated through sequences in the 3′ UTR (Evans et al., 1994; Ogura et al., 2003), which are absent from the *gfp-plk-1* construct that nevertheless results in anterior enrichment (Leidel and Gönczy, 2003). Accordingly, in situ hybridization indicates that *plk-1* mRNA is distributed uniformly in two-cell stage embryos (http://nematode.lab.nig.ac.jp/db2/ShowGeneInfo.php?celk=CELK02520). Therefore, PLK-1 asymmetry is regulated at the protein level. Although other mechanisms can be envisaged, including preferential degradation in the embryo posterior, our findings taken together support a model in which PLK-1 asymmetry is established through preferential PLK-1 protein retention in the embryo anterior.

It will be interesting to investigate the molecular underpinning of PLK-1 anterior retention. Three putative PKC-3 phosphorylation sites are present in PLK-1 (Y.B. and P.G., unpublished) and perhaps phosphorylation of PLK-1 by anteriorly localized PKC-3 contributes to PLK-1 asymmetry. Another possibility is suggested by the observation that PLK-1 distribution is uniform in *nmy-2*(*RNAi*) embryos. Although this may be an indirect consequence from the polarity defects known to arise following NMY-2 depletion (Cuenca et al., 2003; Guo and Kemphues, 1996), the requirement for NMY-2 in PLK-1 localization could be more direct. NMY-2 is enriched on the anterior cortex of one- and two-cell stage embryos (Munro et al., 2004), and may help enrich PLK-1 in the vicinity of

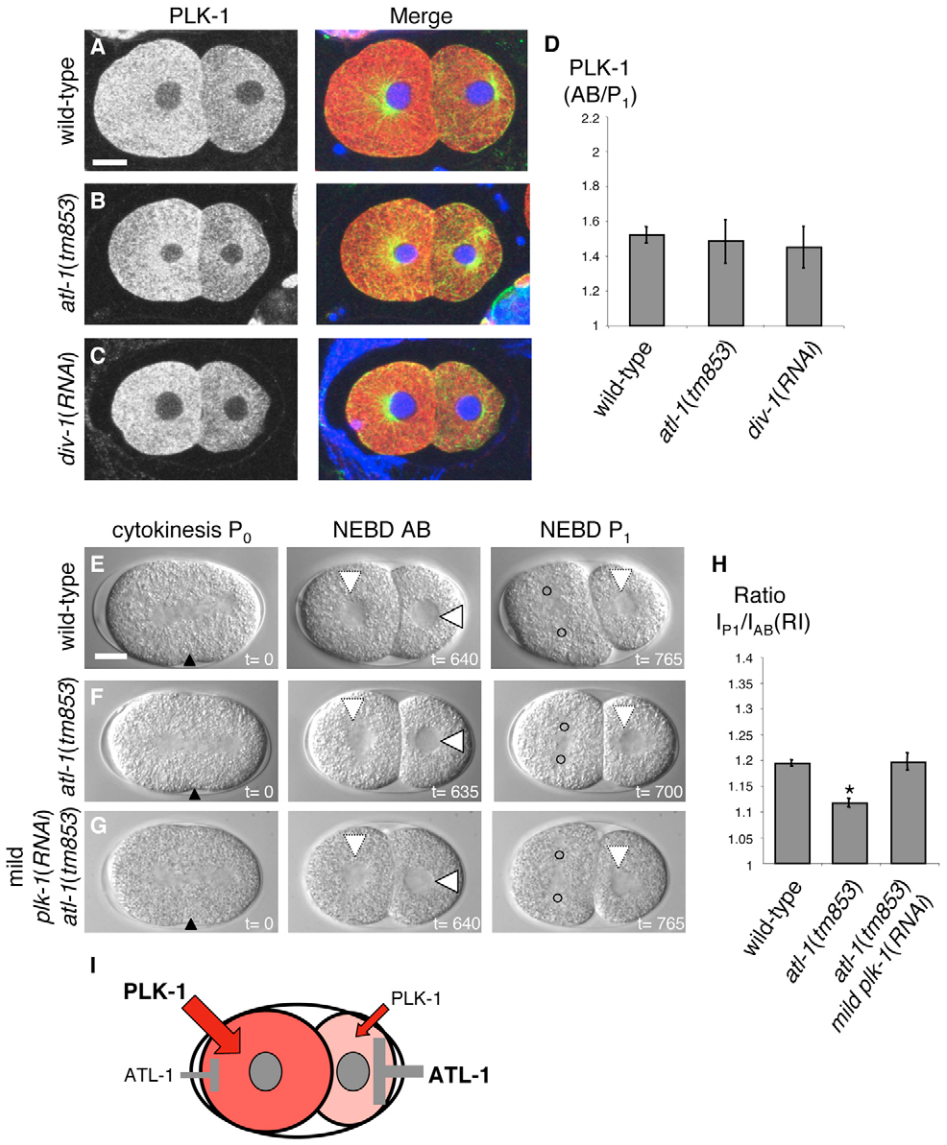

Fig. 7. PLK-1 mediated differential timing is independent of ATL-1. (**A-C**) Wild-type (A), *atl-1*(*tm853*) (B) or *div-1*(*RNAi*) (C) two-cell stage embryo stained for PLK-1 (shown alone in left panels and in red in the merged panels), α-tubulin (green) and DNA (blue). PLK-1 distribution is asymmetric as in the wild type. (**D**) Average ratios, along with s.e.m., of PLK-1 in AB versus P_1 determined on fixed wild-type, *atl-1*(*tm853*) and *div-1*(*RNAi*) embryos. Wild type, 1.52±0.05, *n*=64; *atl-1*(*tm853*), 1.48±0.12, *n*=9, *P*=0.58, compared with the wild type (two-tailed Student's *t*-test); *div-1*(*RNAi*), 1.45±0.17, *n*=8, *P*=0.32, compared with the wild type (two-tailed Student's *t*-test). (**E-G**) Images from DIC time-lapse microscopy of wild-type (E), *atl-1*(*tm853*) (F) or *atl-1*(*tm853*) embryos treated with mild *plk-1*(*RNAi*) (G) (see corresponding Movies 5, 9-10 in the supplementary material). See legend of Fig. 5 for explanation of symbols and timing. (**H**) Average ratios ±s.e.m. of the duration of interphase in P_1 over the duration of interphase in AB [$(I_{P1})/(I_{AB})$] (RI) in embryos of the indicated genotypes. The star denotes that the difference with wild type is statistically significant. See Table S2 in the supplementary material for numerical values and statistical analysis. (**I**) Working model. Preferential promotion of mitotic entry in AB through the presence of more PLK-1, together with preferential retardation of mitotic entry in P_1 through engagement of an ATL-1/CHK-1-dependent checkpoint, ensure differential cell cycle duration in two-cell stage *C. elegans* embryos.

a structure or complex that promotes anterior retention. In *Drosophila*, the non-muscle myosin II Zipper is needed for asymmetric localization of Miranda to the basal side of neuroblasts (Barros et al., 2003).

PLK-1 levels dictate timing of mitotic entry and contribute to asynchronous division in two-cell stage *C. elegans* embryos

Previous work established that PLK-1 is essential for M-phase entry in *C. elegans*, as oocytes from animals severely depleted of PLK-1 do not undergo NEDB or complete the meiotic divisions (Chase et al., 2000). Here, we demonstrate in addition that levels of PLK-1 are important for dictating the timing of mitotic entry. Indeed, partial depletion of PLK-1 delays mitotic entry in AB and more so in P_1, whereas milder depletion of PLK-1 delays mitotic entry merely in P_1.

Where in the cell are the substrates that are phosphorylated by PLK-1 to promote entry into mitosis? Such substrates may reside in the cytoplasm, where PLK-1 enrichment is most apparent. Alternatively, as centrosomes are important for dictating the timing of mitosis in *C. elegans* (Hachet et al., 2007), and as PLK-1 is present at centrosomes, perhaps it is centrosomal PLK-1 that is relevant for mitotic timing. Because centrosomal PLK-1 readily exchanges with PLK-1 in the cytoplasm (Leidel and Gönczy, 2003), an excess of cytoplasmic PLK-1 in the anterior may enhance PLK-1 loading at centrosomes in AB compared with P_1. Accordingly, levels of centrosomal PLK-1 increase during the cell cycle and are high in AB earlier than in P_1 (Y.B. and P.G., unpublished).

Coupling polarity cues and cell cycle progression

Our findings taken together support a model in which two mechanisms together ensure coupling between A-P polarity cues and cell cycle progression in two-cell stage *C. elegans* embryos (Fig. 7I). The first mechanism entails preferential activation of ATL-1/CHK-1 in the P_1 blastomere and contributes to asynchrony by retarding entry into mitosis in P_1 more than in AB (Brauchle et al., 2003). Such preferential checkpoint activation may result from the unequal first cleavage, as preferential activation is largely abrogated in embryos that divide symmetrically. Thus, A-P polarity cues regulate this first mechanism by ensuring asymmetric spindle positioning and unequal cleavage. These earlier findings predicted the existence of another mechanism, also regulated by A-P polarity cues, but independent of size difference and of ATL-1/CHK-1.

Our present work indicates that this second mechanism entails PLK-1 asymmetry, which promotes entry into mitosis in AB earlier than in P_1. The evidence supporting such a mechanism can be summarized as follows. First, PLK-1 is distributed asymmetrically, with more protein present in AB than in P_1. Second, PLK-1 asymmetry is regulated by A-P polarity cues, independently of cell size, as PLK-1 is still asymmetric in *goa-1*/*gpa-16*(*RNAi*) embryos. Third, the time difference between AB and P_1 increases when PLK-1 is depleted, and this occurs in an ATL-1/CHK-1 independent manner. Interestingly, Polo is also asymmetrically distributed in the germarium of *Drosophila*, where it promotes entry into meiosis and oocyte determination (Mirouse et al., 2006). Furthermore, in *Drosophila* neuroblasts, Polo phosphorylates Pon and thus ensures efficient segregation of the fate determinant Numb during asymmetric cell division (Wang et al., 2007). Together with our own work, these findings indicate that the evolutionarily conserved Polo-like kinases may broadly serve to couple cell cycle timing and developmental decisions.

Note added in proof

While this manuscript was under review, another study reported that PLK-1 also regulates MEX-5/6 function (Nishi et al., 2008).

We are grateful to Virginie Hachet, Olivier Hachet and Viesturs Simanis for critical reading of the manuscript, to Kenneth Kemphues and Andy Golden for providing antibodies, to Petr Strnad for help with analyzing the FRAP data, and to Yuji Kohara for in situ hybridization data. For nematode strains, we thank Kenneth Kemphues, Asako Sugimoto, the *Caenorhabditis* Genetics Center, which is funded by the NIH National Center for Research Resources, USA, and the National Bioresource Project, Japan. This work was supported by a grant from Oncosuisse (OCS-01676-02-2005).

Supplementary material

Supplementary material for this article is available at
http://dev.biologists.org/cgi/content/full/135/7/1303/DC1

References

Abrieu, A., Brassac, T., Galas, S., Fisher, D., Labbe, J. C. and Doree, M. (1998). The Polo-like kinase Plx1 is a component of the MPF amplification loop at the G2/M-phase transition of the cell cycle in *Xenopus* eggs. *J. Cell Sci.* **111**, 1751-1757.

Aceto, D., Beers, M. and Kemphues, K. J. (2006). Interaction of PAR-6 with CDC-42 is required for maintenance but not establishment of PAR asymmetry in *C. elegans*. *Dev. Biol.* **299**, 386-397.

Barros, C. S., Phelps, C. B. and Brand, A. H. (2003). Drosophila nonmuscle myosin II promotes the asymmetric segregation of cell fate determinants by cortical exclusion rather than active transport. *Dev. Cell* **5**, 829-840.

Boxem, M., Srinivasan, D. G. and van den Heuvel, S. (1999). The *Caenorhabditis elegans* gene *ncc-1* encodes a cdc2-related kinase required for M phase in meiotic and mitotic cell divisions, but not for S phase. *Development* **126**, 2227-2239.

Boyd, L., Guo, S., Levitan, D., Stinchcomb, D. T. and Kemphues, K. J. (1996). PAR-2 is asymmetrically distributed and promotes association of P granules and PAR-1 with the cortex in *C. elegans* embryos. *Development* **122**, 3075-3084.

Brauchle, M., Baumer, K. and Gönczy, P. (2003). Differential activation of the DNA replication checkpoint contributes to asynchrony of cell division in *C. elegans* embryos. *Curr. Biol.* **13**, 819-827.

Chase, D., Serafinas, C., Ashcroft, N., Kosinski, M., Longo, D., Ferris, D. K. and Golden, A. (2000). The polo-like kinase PLK-1 is required for nuclear envelope breakdown and the completion of meiosis in *Caenorhabditis elegans*. *Genesis* **26**, 26-41.

Colombo, K., Grill, S. W., Kimple, R. J., Willard, F. S., Siderovski, D. P. and Gönczy, P. (2003). Translation of polarity cues into asymmetric spindle positioning in Caenorhabditis elegans embryos. *Science* **300**, 1957-1961.

Cuenca, A. A., Schetter, A., Aceto, D., Kemphues, K. and Seydoux, G. (2003). Polarization of the *C. elegans* zygote proceeds via distinct establishment and maintenance phases. *Development* **130**, 1255-1265.

Edgar, B. A. and O'Farrell, P. H. (1990). The three postblastoderm cell cycles of *Drosophila* embryogenesis are regulated in G2 by string. *Cell* **62**, 469-480.

Encalada, S. E., Martin, P. R., Phillips, J. B., Lyczak, R., Hamill, D. R., Swan, K. A. and Bowerman, B. (2000). DNA replication defects delay cell division and disrupt cell polarity in early *Caenorhabditis elegans* embryos. *Dev. Biol.* **228**, 225-238.

Etemad-Moghadam, B., Guo, S. and Kemphues, K. J. (1995). Asymmetrically distributed PAR-3 protein contributes to cell polarity and spindle alignment in early *C. elegans* embryos. *Cell* **83**, 743-752.

Evans, T. C., Crittenden, S. L., Kodoyianni, V. and Kimble, J. (1994). Translational control of maternal glp-1 mRNA establishes an asymmetry in the *C. elegans* embryo. *Cell* **77**, 183-194.

Garcia-Muse, T. and Boulton, S. J. (2005). Distinct modes of ATR activation after replication stress and DNA double-strand breaks in *Caenorhabditis elegans*. *EMBO J.* **24**, 4345-4355.

Gönczy, P. and Rose, L. (2005). Asymmetric cell division and axis formation in the embryo. In *Wormbook* (ed. The *C. elegans* Research Community), Wormbook, doi/10.1895/wormbook.1.30.1, http://www.wormbook.org.

Gönczy, P., Schnabel, H., Kaletta, T., Amores, A. D., Hyman, T. and Schnabel, R. (1999). Dissection of cell division processes in the one cell stage *Caenorhabditis elegans* embryo by mutational analysis. *J. Cell Biol.* **144**, 927-946.

Gotta, M. and Ahringer, J. (2001). Distinct roles for Galpha and Gbetagamma in regulating spindle position and orientation in *Caenorhabditis elegans* embryos. *Nat. Cell Biol.* **3**, 297-300.

Guo, S. and Kemphues, K. J. (1995). *par-1*, a gene required for establishing polarity in *C. elegans* embryos, encodes a putative Ser/Thr kinase that is asymmetrically distributed. *Cell* **81**, 611-620.

Guo, S. and Kemphues, K. J. (1996). A non-muscle myosin required for embryonic polarity in *Caenorhabditis elegans*. *Nature* **382**, 455-458.

Hachet, V., Canard, C. and Gönczy, P. (2007). Centrosomes promote timely mitotic entry in *C. elegans* embryos. *Dev. Cell* **12**, 531-541.

Inoue, D. and Sagata, N. (2005). The Polo-like kinase Plx1 interacts with and inhibits Myt1 after fertilization of *Xenopus* eggs. *EMBO J.* **24**, 1057-1067.

Kamath, R. S., Fraser, A. G., Dong, Y., Poulin, G., Durbin, R., Gotta, M., Kanapin, A., Le Bot, N., Moreno, S., Sohrmann, M. et al. (2003). Systematic functional analysis of the *Caenorhabditis elegans* genome using RNAi. *Nature* **421**, 231-237.

Kemphues, K. J., Priess, J. R., Morton, D. G. and Cheng, N. S. (1988). Identification of genes required for cytoplasmic localization in early *C. elegans* embryos. *Cell* **52**, 311-320.

Kumagai, A. and Dunphy, W. G. (1996). Purification and molecular cloning of Plx1, a Cdc25-regulatory kinase from *Xenopus* egg extracts. *Science* **273**, 1377-1380.

Lane, H. A. and Nigg, E. A. (1996). Antibody microinjection reveals an essential role for human polo-like kinase 1 (Plk1) in the functional maturation of mitotic centrosomes. *J. Cell Biol.* **135**, 1701-1713.

Leidel, S. and Gönczy, P. (2003). SAS-4 is essential for centrosome duplication in *C. elegans* and is recruited to daughter centrioles once per cell cycle. *Dev. Cell* **4**, 431-439.

Lenart, P., Petronczki, M., Steegmaier, M., Di Fiore, B., Lipp, J. J., Hoffmann, M., Rettig, W. J., Kraut, N. and Peters, J. M. (2007). The small-molecule inhibitor BI 2536 reveals novel insights into mitotic roles of polo-like kinase 1. *Curr. Biol.* **17**, 304-315.

Levitan, D. J., Boyd, L., Mello, C. C., Kemphues, K. J. and Stinchcomb, D. T. (1994). *par-2*, a gene required for blastomere asymmetry in *Caenorhabditis elegans*, encodes zinc-finger and ATP-binding motifs. *Proc. Natl. Acad. Sci. USA* **91**, 6108-6112.

Mirouse, V., Formstecher, E. and Couderc, J. L. (2006). Interaction between Polo and BicD proteins links oocyte determination and meiosis control in *Drosophila*. *Development* **133**, 4005-4013.

Morton, D. G., Roos, J. M. and Kemphues, K. J. (1992). *par-4*, a gene required for cytoplasmic localization and determination of specific cell types in *Caenorhabditis elegans* embryogenesis. *Genetics* **130**, 771-790.

Morton, D. G., Shakes, D. C., Nugent, S., Dichoso, D., Wang, W., Golden, A. and Kemphues, K. J. (2002). The *Caenorhabditis elegans par-5* gene encodes a 14-3-3 protein required for cellular asymmetry in the early embryo. *Dev. Biol.* **241**, 47-58.

Munro, E., Nance, J. and Priess, J. R. (2004). Cortical flows powered by asymmetrical contraction transport PAR proteins to establish and maintain anterior-posterior polarity in the early *C. elegans* embryo. *Dev. Cell* **7**, 413-424.

Murakami, M. S., Moody, S. A., Daar, I. O. and Morrison, D. K. (2004). Morphogenesis during *Xenopus* gastrulation requires Wee1-mediated inhibition of cell proliferation. *Development* **131**, 571-580.

Nishi, Y., Rogers, E., Robertson, S. M. and Lin, R. (2008). Polo kinases regulate *C. elegans* embryonic polarity via binding to DYRK2-primed MEX-5 and MEX-6. *Development* **135**, 687-697.

Ogura, K., Kishimoto, N., Mitani, S., Gengyo-Ando, K. and Kohara, Y. (2003). Translational control of maternal *glp-1* mRNA by POS-1 and its interacting protein SPN-4 in *Caenorhabditis elegans*. *Development* **130**, 2495-2503.

Praitis, V., Casey, E., Collar, D. and Austin, J. (2001). Creation of low-copy integrated transgenic lines in *Caenorhabditis elegans*. *Genetics* **157**, 1217-1226.

Qian, Y. W., Erikson, E., Taieb, F. E. and Maller, J. L. (2001). The polo-like kinase Plx1 is required for activation of the phosphatase Cdc25C and cyclin B-Cdc2 in *Xenopus* oocytes. *Mol. Biol. Cell* **12**, 1791-1799.

Raich, W. B., Moran, A. N., Rothman, J. H. and Hardin, J. (1998). Cytokinesis and midzone microtubule organization in *Caenorhabditis elegans* require the kinesin-like protein ZEN-4. *Mol. Biol. Cell* **9**, 2037-2049.

Roshak, A. K., Capper, E. A., Imburgia, C., Fornwald, J., Scott, G. and Marshall, L. A. (2000). The human polo-like kinase, PLK, regulates cdc2/cyclin B through phosphorylation and activation of the cdc25C phosphatase. *Cell. Signal.* **12**, 405-411.

Rual, J. F., Ceron, J., Koreth, J., Hao, T., Nicot, A. S., Hirozane-Kishikawa, T., Vandenhaute, J., Orkin, S. H., Hill, D. E., van den Heuvel, S. et al. (2004). Toward improving *Caenorhabditis elegans* phenome mapping with an ORFeome-based RNAi library. *Genome Res.* **14**, 2162-2168.

Schierenberg, E. and Wood, W. B. (1985). Control of cell-cycle timing in early embryos of *Caenorhabditis elegans*. *Dev. Biol.* **107**, 337-354.

Sonneville, R. and Gönczy, P. (2004). Zyg-11 and cul-2 regulate progression through meiosis II and polarity establishment in *C. elegans*. *Development* **131**, 3527-3543.

Sumara, I., Gimenez-Abian, J. F., Gerlich, D., Hirota, T., Kraft, C., de la Torre, C., Ellenberg, J. and Peters, J. M. (2004). Roles of polo-like kinase 1 in the assembly of functional mitotic spindles. *Curr. Biol.* **14**, 1712-1722.

Tabuse, Y., Izumi, Y., Piano, F., Kemphues, K. J., Miwa, J. and Ohno, S. (1998). Atypical protein kinase C cooperates with PAR-3 to establish embryonic polarity in *Caenorhabditis elegans*. *Development* **125**, 3607-3614.

Tenenhaus, C., Schubert, C. and Seydoux, G. (1998). Genetic requirements for PIE-1 localization and inhibition of gene expression in the embryonic germ lineage of *Caenorhabditis elegans*. *Dev. Biol.* **200**, 212-224.

Tenenhaus, C., Subramaniam, K., Dunn, M. A. and Seydoux, G. (2001). PIE-1 is a bifunctional protein that regulates maternal and zygotic gene expression in the embryonic germ line of *Caenorhabditis elegans*. *Genes Dev.* **15**, 1031-1040.

Tsang, W. Y., Sayles, L. C., Grad, L. I., Pilgrim, D. B. and Lemire, B. D. (2001). Mitochondrial respiratory chain deficiency in *Caenorhabditis elegans* results in developmental arrest and increased life span. *J. Biol. Chem.* **276**, 32240-32246.

Wang, H., Ouyang, Y., Somers, W. G., Chia, W. and Lu, B. (2007). Polo inhibits progenitor self-renewal and regulates Numb asymmetry by phosphorylating Pon. *Nature* **449**, 96-100.

Watts, J. L., Etemad-Moghadam, B., Guo, S., Boyd, L., Draper, B. W., Mello, C. C., Priess, J. R. and Kemphues, K. J. (1996). *par-6*, a gene involved in the establishment of asymmetry in early *C. elegans* embryos, mediates the asymmetric localization of PAR-3. *Development* **122**, 3133-3140.

Watts, J. L., Morton, D. G., Bestman, J. and Kemphues, K. J. (2000). The *C. elegans* par-4 gene encodes a putative serine-threonine kinase required for establishing embryonic asymmetry. *Development* **127**, 1467-1475.